Physical Science International Journal

25(3): 9-17, 2021; Article no.PSIJ.69702
ISSN: 2348-0130

Magnetoresistance Recovery in the Amorphous Dielectric Material SiCOH

Philip A. Williams[1*] and James R. Lloyd[2]

[1]*College of Nanoscale Science and Engineering, State University of New York at Albany, 1400 Washington Avenue, Albany, 12222, New York, US.*
[2]*College of Nanoscale Science and Engineering, State University of New York Polytechnic Institute 257 Fuller Road, Albany, 12203-New York, US.*

Authors' contributions

This work was carried out in collaboration between both authors. All authors read and approved the final manuscript.

Article Information

DOI: 10.9734/PSIJ/2021/v25i330245
Editor(s):
(1) Dr. Lei Zhang, Winston-Salem State University, USA.
(2) Dr. Thomas F. George, University of Missouri-St. Louis, USA.
Reviewers:
(1) Akarsh Verma, University of Petroleum and Energy Studies, India.
(2) Pruthviraj. R. D, VTU, India.
(3 Jaime Thissen, University of Illinois Urbana-Champaign, USA.
Complete Peer review History: http://www.sdiarticle4.com/review-history/69702

Original Research Article

Received 06 April 2021
Accepted 16 June 2021
Published 19 June 2021

ABSTRACT

The use of a magnetoresistance in the characterization of transport properties in the amorphous low-k dielectric material SiCOH is demonstrated. The double occupancy of charge carriers in trap states within the dielectric material can only exist in spin singlet formation due to Pauli Exclusion. The trap-assisted negative magnetoresistance (MR) in amorphous SiCOH, driven by an applied electric field that results in an observed increase in magnitude of the current in the conduction band is due to singly occupied trap spin-mixing suppression of carriers with the application of an external magnetic field. The material MR decays with time under electrical bias and temperature stress as traps are filled by charge carriers and from space charge accumulation. The MR can be reinstated by the ionization of these traps via the conduction mechanisms of nonthermally activated tunneling and thermal ionization with the assistance of an applied coulombic potential barrier lowering electric field. In this work a direct correlation is shown between a material MR and the trapping, de-trapping, and avoidance of spin-singlet state trap formations in the transport of charge carriers in the amorphous low-k dielectric material SiCOH (a-SiCOH).

**Corresponding author: E-mail: Pwilliams@albany.edu;*

Keywords: Dielectric breakdown; dielectric materials; magnetic materials; magnetoresistance, hyperfine.

1. INTRODUCTION

There has long been an interest in the carrier transport properties of dielectric materials for obvious reasons. Dielectric materials are insulators that have been used in the fabrication of integrated circuits to electrically isolate conductors and in capacitors. Dielectrics have a large energy bandgap with the ability of the atoms within the dielectric material to become polarized by an applied electric field and store electrical charge. The introduction of low-k dielectrics in industry was an effort to reduce the RC response time inherent in dielectric materials used as electrical insulators. Low-k dielectric materials such as SiCOH have been instrumental in achieving that goal and are currently used as an intermetal dielectric (IMD) insulating material, and in metal-insulator-metal (MIM) Resistive Random-Access-Memory (ReRAM) cells for nonvolatile memory, as well as in CMOS applications [1,2].

The interlevel low-k dielectric leakage currents can become appreciable with the application of relatively large electric fields and are a detriment to Integrated Circuit (IC) device performance [3]. The leakage currents in dielectrics are believed to ultimately contribute to device insulation degradation and failure rates in time dependent dielectric breakdown (TDDB). Moreover, the study of dielectric material defect related trapping and emission of charge carriers are important in understanding 1/f noise in IC devices, and as internode dimensions further decrease, is also believed to result in unwanted random telegraph noise [4]. The use of a material MR that can be easily acquired at room temperature to help elucidate the role of various conduction mechanisms and defects (traps) within the bulk dielectric of the material that results in TDDB failures, could be instrumental. Therefore, the study of the conduction mechanisms in dielectric materials used as electrical insulators are of great importance in understanding material changes and failure rates due to TDDB [5].

In this study, interdigitated comb capacitor TDDB structures were used with an applied magnetic field to probe the electrical conduction mechanisms and the role of defects within the dielectric material [6]. The negative MR in a-SiCOH results in an increase in the current within the conduction band of the low-k dielectric under electric field bias with the application of a magnetic field. The material MR is determined by taking the difference between the interelectrode bulk dielectric material current from the magnetic field *(H)* induced dielectric conduction current $\Delta I = I(H) - I(0)$, which is then normalized by the interelectrode bulk dielectric current devoid of the applied external magnetic field, $I(0)$. The magnitude of the material MR is independent of the orientation of the applied external magnetic field with respect to the direction of current flow in the dielectric film. The MR effect is also seen in organic semiconductors (OMAR) by inhibiting bipolaron formation with the application of a relatively modest magnetic field [7,8].

2. METHODOLOGY

The dielectric material transport properties were studied using the low-k dielectric material a-SiCOH due to its inherent negative MR and the film was fabricated into metal-insulator-metal (MIM) interdigitated comb capacitor structures. The electrodes were composed of Cu with a 3 nm Ta/TaN barrier lining in direct contact with the a-SiCOH material with a nominal spacing of 40 nm between electrodes [6]. The width of each comb capacitor finger comprising the interdigitated structure was 40 nm, totaling 5000 fingers in all for each structure. The samples were mounted, and wire bonded to dual inline packages (DIPs), and the MR of each comb capacitor DIP structure was measured at room temperature. The external magnetic field source used in this experiment was from a solenoid measured at a modest 100 Gauss (100 Oersted). The DIPs were pre-screened with and without the inclusion of magnetic liner materials such as nickel, as well as for other underlying ferromagnetic materials with no apparent differences. The samples used in this work were obtained from the same ingot material wafer to avoid any fabrication and material variations.

Fig. 1. Displays the initial MR measurement curve of one DIP structure sample where in section 1 and 3 the structure current is measured devoid of the applied external magnetic field and in section 2 the MR measurement is obtained with the magnetic field applied. In Fig. 2, the MRs of a single DIP structure sample were initially obtained from a MR measurement series using bias voltages from 12 – 15 V (3 – 3.75 MV/cm), in steps of one Volt, and again at 13 Volts at the

completion of the bias voltage series for later comparison. The DIP structure background and differential current of the MR measurement series is displayed in Table 1. The DIP sample of Fig. 1 was taken from the same wafer, as were all of the samples used here, and the MR was initially obtained at 14 V (3.5 MV/cm) before the sample was subjected to bias voltage and temperature stress (BTS) accelerated testing for a total of 473 hours at a bias voltage of 14 V, and a temperature of 125 ^{0}C. At the end of the BTS accelerated testing, the sample was extracted, allowed sufficient time to cool, and serial measurements of MR were retaken at room temperature at bias voltages of 14 V, 16 V, and again at 14 V. The results of the serial MR measurements are illustrated in the bar chart of Fig. 3, with associated background current and differential current displayed in Table 2.

Initial magnetoresistance pre BTS at room temperature

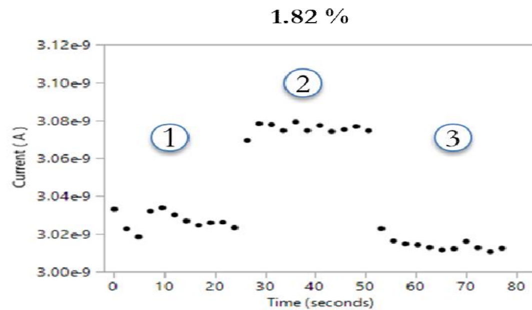

Initial magnetoresistance observed at 14v (3.5 MV/cm) at 25 ^{0}C.
E-Field 3.5 MV/cm, Sample width dimension 40 nm

Fig. 1. Initial single sample MR before 473 hours of accelerated testing to be later stressed at 14V and 125 ^{0}C. An applied bias voltage of 14V and a magnetic field of 100 Gauss was applied externally at room temperature (~25 ^{0}C) and the MR is as indicated. The magnetic field in areas 1 and 3 is off and in area 2 the magnetic field is switched on

Single sample magnetoresistance series at room temperature

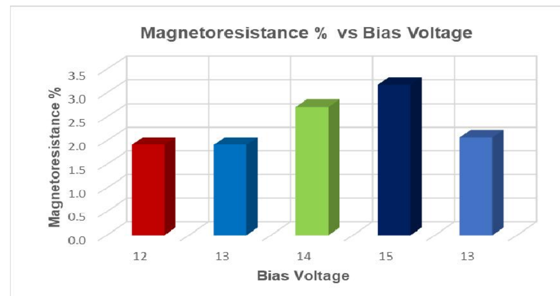

Fig. 2. Single sample MR voltage bias continuous series at room temperature (~25 ^{0}C). Here the MR measured at a 14 V bias is nearly replicated at the end of the series

Table 1. Bias voltage and percent magnetoresistance. The current is the interelectrode current in amperes and Delta ILD is the change in current

Bias Voltage	Magnetoresistance %	Current (A)	Delta ILD (A)
12	1.91	3.50E-10	6.70E-12
13	1.91	1.17E-9	2.23E-11
14	2.71	3.48E-9	9.44E-11
15	3.17	9.58E-9	3.04E-10
13	2.07	1.05E-9	2.19E-11

Some of the samples that did not undergo accelerated testing were subjected to continuous periodic MR testing, and data acquired after an initial 300 second idle time-period prior to measurement, obtained in series intervals of: 90, 105, and 180 seconds respectively, and the results are shown in Fig. 5.

3. RESULTS

Fig. 2 displays a bar chart illustrating an increase in the magnitude of the MR of the dielectric material a-SiCOH with increased bias voltage, 12 – 15 V, taken in steps of one volt. There is a slight increase in the magnitude of the MR when replicated at a 13 V bias indicated at the end of the measurement series. We attribute this to subsequent damage to the dielectric material after having been subjected to increased bias voltages. As a result of this, the MR of the dielectric material a-SiCOH does not always decay during BTS testing as trap occupancy increases if there is sufficient elastic and or inelastic impact scattering of electrons imparting their energy and momentum in part to atoms within the dielectric. This causes further damage and increases the number of defects (traps) within the material [5]. There is a finite probability that an electron could gain enough kinetic energy under the influence of an applied electric field to displace a hydrogen atom within the a-SiCOH dielectric thereby creating a newly available dangling bond defect (trap) if the electron travel exceeds the critical distance damage threshold for the material [5]. The probability that an electron will gain sufficient energy to reach the dielectric material damage threshold is the probability that the electron travel λ will exceed its mean-free path μ through the dielectric material, which is approximately 1 nm for low-k dielectrics, and is relatively independent of the applied electric field E,

$$\mathrm{P}(\mathcal{E}_{\lambda} > \mathcal{E}_{\mathrm{t}}) = \mathrm{e}^{-\mathcal{E}_{\mathrm{t}}/\mu \mathrm{e} \mathrm{E}} = \mathrm{e}^{-\lambda_{\mathrm{t}}/\mu} \quad (1)$$

$$\lambda_t = \frac{\mathcal{E}_t}{eE} \quad (2)$$

$$\mathrm{P}(\lambda > \lambda_{\mathrm{t}}) = \mathrm{e}^{-\lambda_{\mathrm{t}}/\mu} \quad (3)$$

where $\mathcal{E}_{\lambda}$ is the electron energy inside the dielectric, $\mathcal{E}_t$ is the energy required to break the chemical bond and completely dissociate an atom of hydrogen, and λ_t is the minimum distance that the electron must traverse to cause damage within the dielectric material [5]. However, in the absence of this, the MR will otherwise decay with increased carrier trap occupancy and as more space charge accumulates within the dielectric material [9,10].

Some of the test structures that underwent BTS accelerated testing for 473 hours were extracted from the chamber, allowed to cool to room temperature (25 ^{0}C), and their MRs were retaken, where the initial pre-BTS MR magnitude of Fig. 1 is displayed in Fig. 3A. In these test structures a MR was not observed post BTS when subjected to a bias of 14 V as shown in Fig. 3B, and this is most likely due to having achieved sufficient trap-filling from space charge accumulation. However, upon increasing the bias to 16 V, a MR reemerged and is shown in Fig. 3C. The larger MR observed at higher bias voltages is attributed to more charge carriers having been injected into the conduction band thereby increasing the probability of charge carriers becoming trapped in previously empty and singly occupied traps located below the conduction band devoid of a magnetic field, and then selectively avoiding the singly occupied traps due to double occupancy spin-mixing constraints during the application of the magnetic field [6]. Lastly, the MR was again measured at the lower 14 V bias and the results are displayed in Fig. 3D. The MR in Fig. 3D is lower than the original pre-BTS MR of Fig. 3A, measured at the very same bias voltage, that is displayed in Fig. 1. This can be attributed in part to the Poole-Frenkel (field-assisted thermal ionization) coulombic trap barrier lowering effect that an electric field has on traps within the bulk dielectric material [11-13] at the much higher bias voltage used, enabling some of the charge carriers to escape from shallow traps making them again available for occupancy at lower bias voltages as shown in Fig. 4. Thus, the trap (defect) potential barrier energy will be lowered by an amount $\Delta\Phi_{PF}$ provided by the Poole-Frenkel relation.

$$\Delta\Phi_{PF} = \beta_{PF} E^{\frac{1}{2}} \quad (4)$$

$$\beta_{PF} = \sqrt{\left(\frac{e^3}{\pi\kappa\epsilon_0}\right)} \quad (5)$$

Where E is the applied electric field, κ is the dielectric constant, and ϵ_0 is the free-space

permittivity, and e is the charge of an electron, and β_{PF} a constant as shown. The other contributing factor to the resulting MR observed is due to the subsequent material damage sustained at the previous higher bias voltage [5], creating newly available traps for occupancy within the insulator. We note that all of the traps inside the insulator will never be completely filled with carriers below the trap-filled limit (TFL) voltage of the material as opposed to instead having established a steady-state condition of random telegraph noise resulting from the constant trapping and emission of charge carriers mostly from shallow traps [4,14].

Single sample magnetoresistance measurements at room temperature

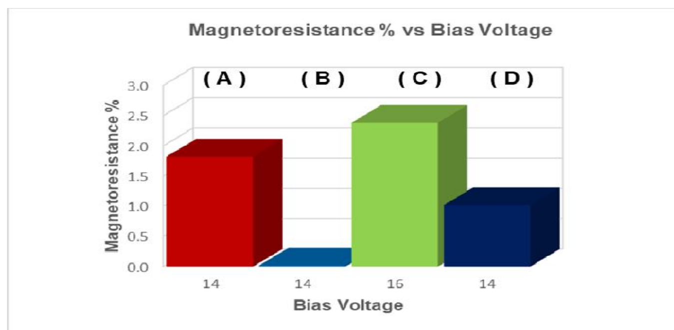

Initial magnetoresistance observed at 14v (3.5 MV/cm) at 25^{0}C

Fig. 3. Single sample MR voltage biased from 14 – 16 V at room temperature (~25 ^{0}C). Initially, the MR in (A) at a 14 V bias later vanishes post BTS testing for 473 hours at 125 ^{0}C in (B). In (C) the MR is measured at a 16 V bias and recovered. A MR is then again observed at the 14 V lower bias voltage post 16 V bias testing as shown in (D)

Table 2. Bias voltage and percent magnetoresistance. The current is the interelectrode current in amperes and Delta ILD is the change in current

Bias Voltage	Magnetoresistance %	Current (A)	Delta ILD (A)
14	1.82	3.02E-9	5.50E-11
14	0.02	1.08E-8	2.99E-11
16	2.38	1.97E-8	4.68E-10
14	1.02	4.22E-9	4.29E-11

Poole-Frenkel Effect – Field Assisted Thermal Ionization

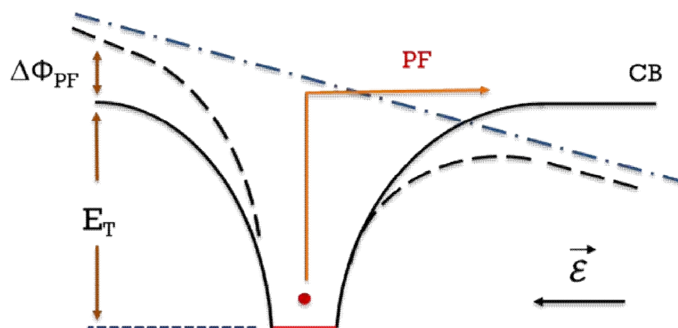

Fig. 4. Energy diagram of a donor trap center in the presence of the electric field indicated by the curved dashed lines. The PF arrow indicates the mechanism of electron emission: thermal ionization over the lowered barrier (PF effect) into the conduction band (CB)

The remaining test structures that were subjected to continuous periodic MR series testing after a latent period of 300 seconds exhibited periodic vacillations as shown in Fig. 5A. We note that the periodicity of the MR curve was induced by intermittently switching the externally applied magnetic field on and off during each measurement in the set 90 second time interval and is not a function of the material itself. However, the magnitude of the MR vacillation appears to be a function of trap density and occupation availability in the material and is commensurate with the measurement interval periodicity. Moreover, the amplitude of the vacillation increases in the second 180 second time interval as shown. In Fig. 5B the MR measurement periodicity was increased to 105 seconds and a vacillation amplitude attenuation in the MR magnitude is observed with time after the initial 105 second time interval and remains relatively constant. In Fig. 5C the MR measurement interval is further increased to 180 seconds and the vacillation amplitude further decreases and remains almost relatively constant as in the previous case. The observed phenomenon is due to a perturbation in the trapping of charge carriers in the dielectric material induced by the intermittently applied external magnetic field. Moreover, the 300 – 400 second latent time-period before testing is required to allow adequate time for sufficient charge trapping and to achieve steady-state conditions representative of a leakage current as opposed to a displacement current, otherwise the MR magnitude vacillation was not observed.

Trap Assisted Magnetoresistance Percentage Fluctuations with Time

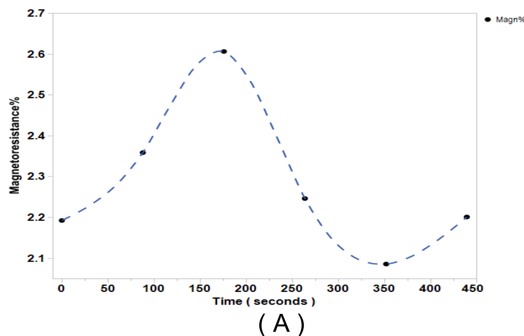

(A)

Fig. 5A. Delayed MR measurements of 300 seconds at 13 volts and 90 second intervals. MR % versus time (sec)

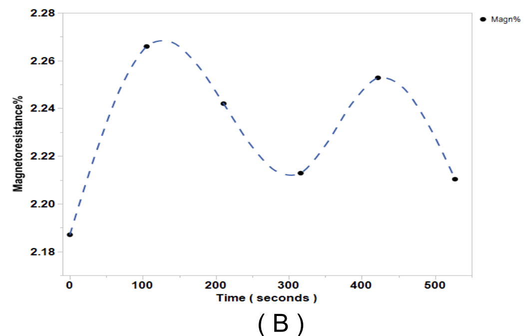

(B)

Fig. 5B. Delayed MR measurements of 300 seconds at 13 volts and 105 second intervals. MR % versus time

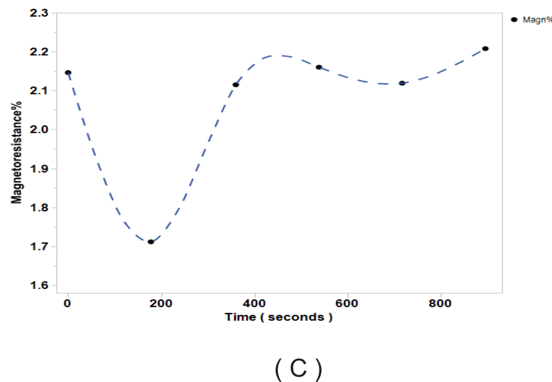

(C)

Fig. 5C. Delayed MR measurements of 300 seconds at 13 volts and 180 second intervals. MR % versus time (sec)

Fig. 5. Series magnetoresistance measurement fluctuates in time post 5-minute stress bias voltage latent time-period with no magnetic field applied

Fig. 6A displays a typical MR magnitude curve as a function of time. As illustrated in the graph, the MR increases with time and then eventually saturates for a duration of time. Since there is no apparent change in the magnitude of the MR in the saturation range, one need only wait to measure the MR when in that range, which is typically about 100 – 150 seconds. Fig. 6B is a dual axis graph of the magnitude of the MR and the corresponding average background current as a function of time. As shown, the average background current decreases as the magnitude of the MR increases. The background current as defined here is the measured average current in the dielectric material obtained just before and after the magnetic field is applied.

4. DISCUSSION

Hydrogen nuclei in the dielectric material a-SiCOH are thought to promote spin-mixing of triplet-singlet two-electron spin states via a hyperfine interaction due to the randomly oriented magnetic moments of hydrogen nuclei inside the material [8]. The MR in the dielectric material a-SiCOH is due to the spin-polarizing cooperative effect of electrons from an applied external magnetic field resulting in the suppression of triplet to singlet transitions of electrons [6,7]. This then results in a rise in current within the conduction band of the dielectric material a-SiCOH due to a suppression of singlet state formations of electrons in localized electronic trap states due to Pauli Exclusion and shorter triplet trapping times with the application of an external magnetic field.

The two basic conduction mechanisms in dielectric materials are bulk-limited conduction and electrode-limited conduction, wherein the former involves the electrical properties of the bulk dielectric material and the latter the physical properties of the electrode-dielectric interface. The predominant conduction mechanisms of the low-k dielectric material a-SiCOH are known to either be Schottky (Thermionic) or Poole-Frenkel emission (PFE), or a combination thereof. In bulk limited conduction, PFE is characterized by a trap-assisted transport mechanism of charge carriers through thermal excitation and the subsequent emission of carriers from traps hopping between nearest neighbor trap sites and is described elsewhere [3,11,14]. The hopping frequency of carriers can decrease if there is not a readily available energy state for electron occupancy. However, at some point after a sufficient number of traps have been filled, a material MR is no longer observed and the current between electrodes in the a-SiCOH dielectric material increases approximately

Series MR measurements commence after a 10 s delay prior to first measurements with no external magnetic field applied during latent periods

Magnetoresistance Percentage series measurements

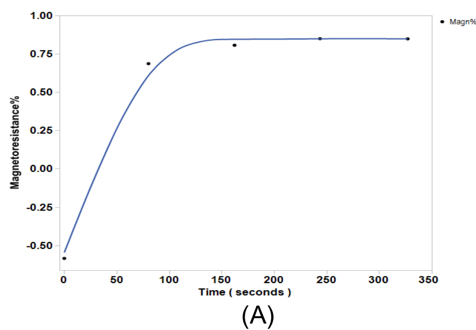

(A)

14 Volt bias (E-Field 3.5 MV/cm) and at 80 Second Intervals

Fig. 6A. Displays a typical MR magnitude series curve as a function of time. As illustrated in the graph, the MR increases with time and then eventually saturates for a duration of time

Magnetoresistance percentage vs. Background current

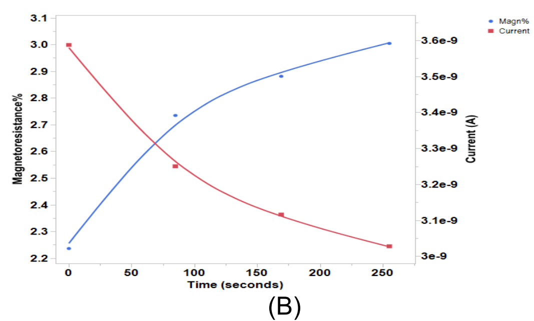

(B)

Bias voltage 13V and E-Field 3.25 MV/cm

Fig. 6B. There is an inverse relationship between the current in the dielectric and the magnitude of the MR of the material (blue : MR, red : current)

tenfold. Once a MR is reestablished in the material the current summarily drops by about the same factor. Insulators with inherent material defects (traps) will reach a transition point if sufficient charge is injected into the material and as a result space charge limited (SCL) conduction occurs governed by the Mott Gurney trap-mediated equation [14]. Moreover, if the injected free-carrier current density exceeds the volume generated free-carrier density, then SCL conduction will predominate. Thus, at the TFL any additional subsequent injected charge will contribute to the current as free electron charge in the conduction band of the material. Beyond the TFL, the conduction mechanism will be governed by the Mott and Gurney equation for defect-free SCL conduction [14]. The transition from PFE to SCL conduction could be a contributing factor to TDDB in low-k dielectrics suggesting a charge to failure threshold, but more investigation is needed.

5. CONCLUSION

The study of material defects (traps) and their contribution to leakage currents in dielectric materials used as insulators to isolate conductors in the back-end-of-the-line and transistors in the front-end-of-the-line is essential to the understanding of dielectric breakdown. Thus, the use of a trap-assisted material MR could be a novel and informative way to further elucidate the role of conduction mechanisms and defect densities in low-k dielectric materials such as a-SiCOH in TDDB device failure rates.

DISCLAIMER

The products used for this research are commonly and predominantly use products in our area of research and country. There is absolutely no conflict of interest between the authors and producers of the products because we do not intend to use these products as an avenue for any litigation but for the advancement of knowledge. Also, the research was not funded by the producing company rather it was funded by personal efforts of the authors.

ACKNOWLEDGMENTS

The authors would like to thank IBM Corporation for providing the samples, Patrick Lenahan of Penn State University for providing peripheral materials, and to acknowledge DARPA/BOEING for their funding and support of this work.

COMPETING INTERESTS

Authors have declared that no competing interests exist.

REFERENCES

1. Ye Fan, Sean W. King, et al., Characterization of Porous BEOL Dielectrics for Resistive Switching, The Electrochemical Society, ECS Transactions. 2016;72(35):2.
2. Mikhail R. Baklanov, Martin L. Green, Karen Maex, Dielectric Films for Advanced Microelectronics, Electrical Characteristics of Advanced Gate Dielectrics, Copyright John Wiley & Sons Ltd., The Atrium Southern Gate, Chichester, West Sussex PO19 89Q, England. 2007(1):252, 376.
3. Fu-Chien Chiu, A Review on Conduction Mechanisms in Dielectric Films, Department of Electrical Engineering, Ming Chuan University, Taoyuan 333, Taiwan. Received 29 August 2013; Revised 5 December 2013; Accepted 11 December 2013; Published 18 February 2014.
4. Van Der Ziel A. Unified Presentation of 1/f Noise in Electron Devices: Fundamental 1/f Noise Sources, Proceedings of the IEEE. 1988;76(3).
5. Lloyd JR. Lucky Electron Model for TDDB in Low-k Dielectrics, SUNY Polytechnic Institute, College of Nanoscale Science and Engineering, 257 Fuller Road, Albany, NY 12203, USA, IEEE Transactions on Device and Materials Reliability. 2016;16(4):1-1 2619071.
6. McGowan BT, Lloyd JR. Negative Magnetoresistance in a Low-k Dielectric, College of Nanoscale Science and Engineering, SUNY Polytechnic Institute, 257 Fuller Road, Albany, NY 12203, USA, Journal of Applied Physics Letters. 2014;105, 252902.
7. Harmon NJ, Flatte ME. Organic Magnetoresistance from Deep Traps, Department of Physics and Astronomy and Optical Sciences and Technology Center, University of Iowa, Iowa City, Iowa, USA, Department of Applied Physics, Endhoven University of Technology, P.O. Box 513, 5600 MB, Endhoven, The Netherlands, Journal of Applied Physics; 2014.
8. Wagemans W, Janssen P, et al. The Many Faces of Organic Magnetoresistance,

World Scientific SPIN. 2011;01(01):93 – 108.

9. McGowan BT, Lloyd JR. Decay of Magnetoresistance in a Low-k Dielectric Upon Application of Electrical Bias and Temperature Stress, College of Nanoscale Science and Engineering SUNY Polytechnic, Albany NY USA, Publisher IEEE International Integrated Reliability Workshop (IIRW), Conference Oct; 2015.
10. McGowan BT, Nolting WM, Lloyd JR. Effects of Electrical Bias and Temperature Stress on the Negative Magnetoresistance of a Low-k Dielectric, College of Nanoscale Science and Engineering, SUNY Polytechnic Institute, 257 Fuller Road, Albany, NY 12203, USA, Journal of Applied Physics. 2015;118:224106.
11. Aditya Guha, A Review of Frenkel-Poole Emission, International Journal of Electrical and Electronic Engineers. 2015;7(02).
12. Bertulani CA. Tunneling of atoms, nuclei, and molecules, Department of physics and Astronomy, Texas A&M University-Commerce, Springer, Few Body Systems. 2015;(56):727-736.
13. Simmons JG. Richardson-Schottky Effect in Solids, Electrical Engineering, University of Toronto, Toronto, Canada, Phys. Rev. Letters. 1965;15;967(15).
14. Simmons JG. Handbook of Thin Films, “Electronic Conduction Through Thin Insulating Films,” Chapter Edited by Leon I. Maissel, Reinhard Glang, IBM Corporation, Components Division, East Fishkill Facility, Hopewell Junction, NY, McGraw Hill Incorporated. 1970;14:1-37.

© 2021 Williams and Lloyd; This is an Open Access article distributed under the terms of the Creative Commons Attribution License (http://creativecommons.org/licenses/by/4.0), which permits unrestricted use, distribution, and reproduction in any medium, provided the original work is properly cited.

Peer-review history:
The peer review history for this paper can be accessed here:
http://www.sdiarticle4.com/review-history/69702